Electron-energy-loss spectroscopy of core levels and valence-band region in cerium and cerium dioxide

J. Bloch, N. Shamir, M. H. Mintz, and U. Atzmony
Nuclear Research Center—Negev, P.O. Box 9001, Beer-Sheva 84190, Israel
(Received 29 July 1983; revised manuscript received 12 December 1983)

Electron-energy-loss spectra of sputtered clean cerium metal and of cerium dioxide were measured in the valence-band region and in the vicinities of the $4d$, $4p$, $4s$, $3d$, and $3p$ excitation thresholds. The energies of the primary electrons ranged from 80 to 3000 eV. Bulk and surface plasmons were identified in the valence-band region of the metal. For the dioxide, the surface plasmon vanished and "plasmonlike" peaks were observed. Also, an intra-conduction-band transition which appears in the metal and is highly sensitive to the chemical state of the surface was found. Core-level excitations were identified as transitions to the $4f$ levels located above, within, and below the conduction band. Transitions of the $4d$ electrons displayed "giant resonances" due to the higher multiplet splittings of the final states. The intensities of some of the excitation lines were enhanced at low incident electron energies due to the contribution of higher multipole transitions. The core-level excitations were also found in the oxide. Chemical shifts of some of the oxide peaks relative to those of the metal were observed, especially for transitions into final states located above the metallic conduction band.

I. INTRODUCTION

Transmission-mode electron-energy-loss spectroscopy (ELS) studies have been used to investigate the valence-band region[1] and the $4d$ excitations[2] of rare-earth metals and compounds. Many features common to all rare-earth elements were found. They were interpreted on the basis of similar electronic configurations of these elements. Recently, some rare-earth systems were studied by reflection ELS.[3–5] The latter studies were carried under better UHV conditions and a higher resolution. Additional features were revealed, especially in the low-energy range, and some surface effects were observed.[6] Excitations of core levels other than the $4d$ were not studied in detail by the ELS technique. The $4d$ (Refs. 7 and 8) and the $3d$ (Ref. 9) core-level excitations of Ce metal and some of its compounds were studied by x-ray absorption technique and the results were partially interpreted by the atomic physics approach.[10] In contrast to the other rare-earth systems the Ce transitions displayed distinct dependence of the spectra on the chemical environment.

In this paper we present ELS studies of Ce and CeO_2 over a range of energy loss extending from the valence-band region to the vicinity of the $3p$ threshold. Some features of the spectra are analyzed. The dependence on the primary electron energies and the chemical shifts of some of the lines are considered in order to separate surface and bulk effects.

II. EXPERIMENTAL

The experimental system used was a PHI spectrometer model no. 548 with a base pressure of 2×10^{-8} Pa. An electron beam (80—3000 eV) from an electron gun impinged on the sample surface, was backscattered and detected by a coaxial cylindrical mirror analyzer (CMA)

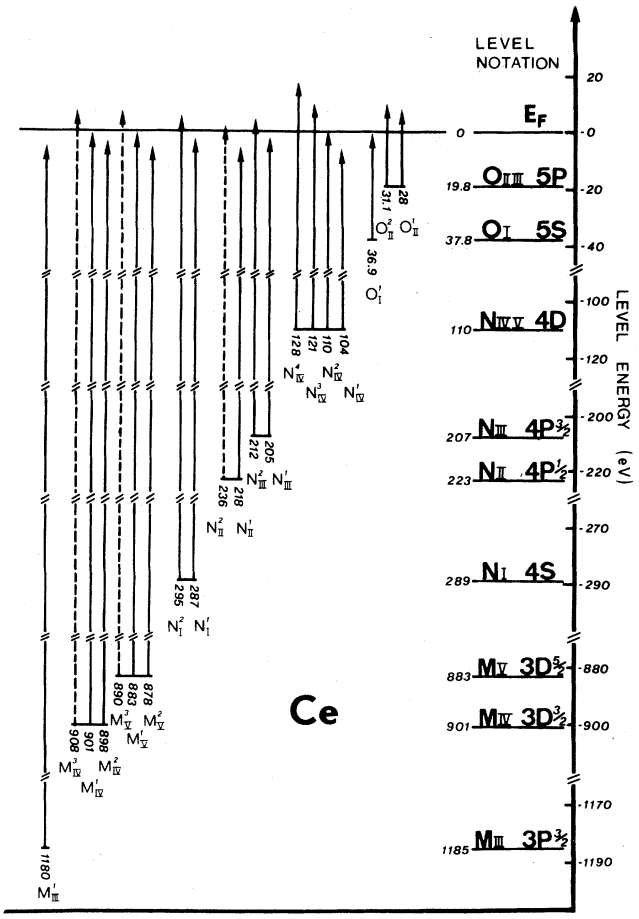

FIG. 1. Electronic energy-level diagram (Ref. 11) and the electron-energy-loss transitions of Ce metal. Dashed lines indicate a very low intensity transition.

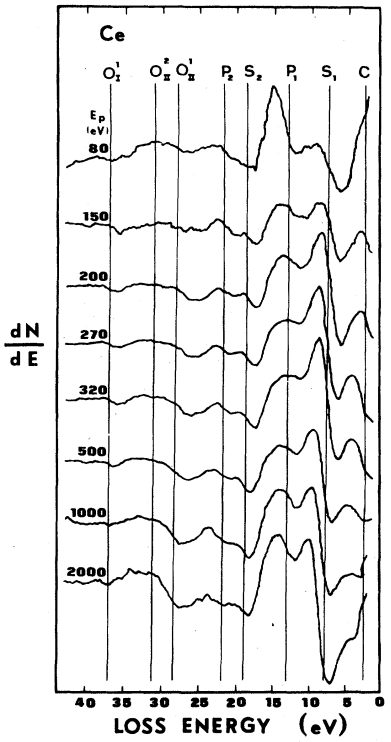

FIG. 2. Electron-energy-loss spectra of sputtered cerium metal in the valence-band region for various incident electron energies (E_p).

PHI model no. 15-255 G that was operated at constant resolving power: pass energy of 50 eV and modulation of 1-V peak to peak for the valence-band region ($\Delta E \leq 50$ eV) and pass energy of 200 eV and modulation of 2 V for the higher ranges. The first-derivative spectra were recorded using a lock-in amplifier. Ar^+-ion gun with beam energies up to 5 keV was incorporated in the system for sputter etching of the specimen surface. It could be

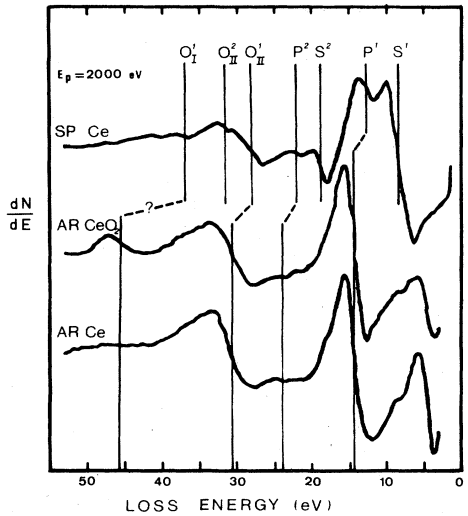

FIG. 3. Electron-energy-loss spectra of SP Ce, AR CeO_2, and AR Ce in the valence-band region.

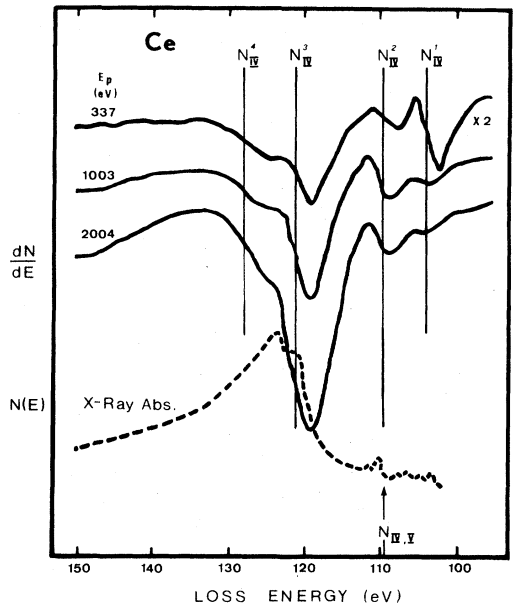

FIG. 4. Electron-energy-loss and x-ray absorption (Ref. 7) spectra in the vicinity of the $4d$ ($N_{IV,V}$) transition range of cerium metal (SP Ce).

operated simultaneously with the recording of the ELS. Thin slices of cerium metal were cut from 99.9%-pure Ce ingot, and cleaned with CCl_4 before being introduced into the UHV chamber. These samples will be referred to as "as-received Ce" (AR Ce). Cleaned metallic Ce surfaces were obtained by Ar^+ bombardment and will be referred to as "sputtered Ce" (SP Ce). The ELS of the SP Ce were taken while simultaneously sputtering the sample with 4.5 keV Ar^+. Auger electron spectroscopy (AES) measurements of the SP Ce indicated that the only contaminants that remained were chlorine and oxygen with atomic concentrations below 0.8%.

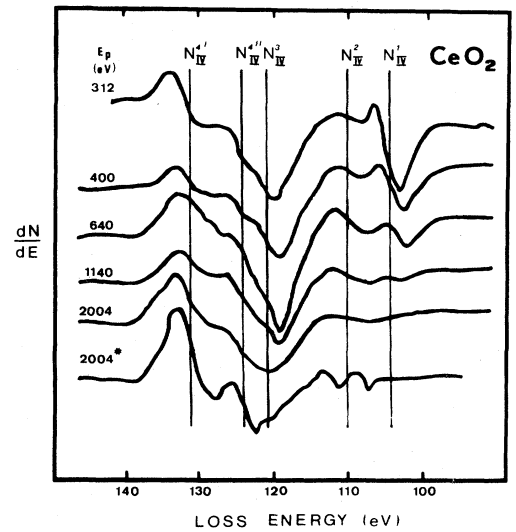

FIG. 5. Electron-energy-loss spectra in the vicinity of the $4d$ transition range of CeO_2. The asterisk indicates higher resolution conditions.

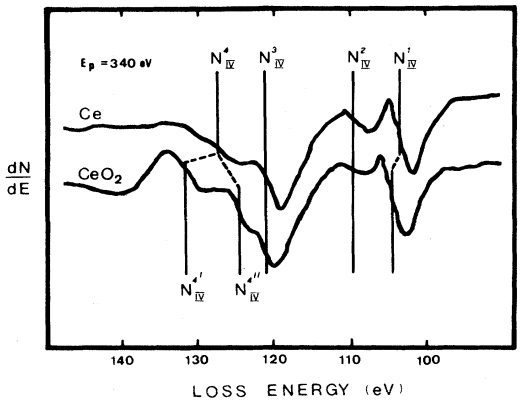

FIG. 6. Electron-energy-loss spectra of SP-Ce and CeO_2 near the $4d$ transition range for relatively low incident-electron energy.

CeO_2 samples were prepared by pressing the corresponding powder (graded as "specpure" with the total of rare-earth impurities less than 100 ppm and other impurities less than 20 ppm) onto an indium foil and cleaning with CCl_4. This sample will be referred to as "as-received CeO_2" (AR CeO_2). AES did not reveal any distinguishable differences between the AR CeO_2 sample and the AR Ce. This indicates the existence of a heavily oxidized layer on the AR Ce. On the other hand, x-ray photoelectron spectroscopy (XPS) measurements[11] revealed the presence of additional trivalent Ce species on the surface of the passivated Ce metal.

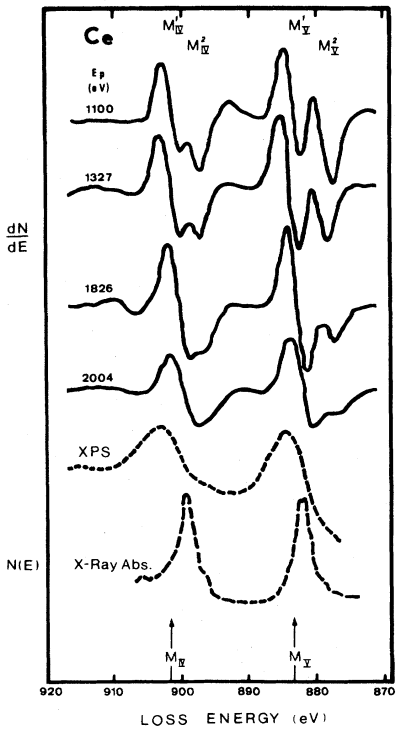

FIG. 7. Electron-energy-loss, x-ray photoelectron, and x-ray absorption (Ref. 14) spectra in the vicinity of the $3d_{3/2}(M_{IV})$ and the $3d_{5/2}(M_V)$ transition range of SP Ce.

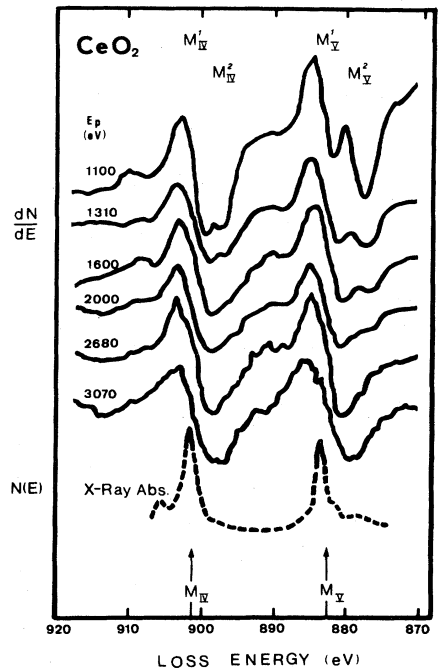

FIG. 8. Electron-energy-loss and x-ray absorption (Ref. 9) spectra in the vicinity of the $3d_{3/2}(M_{IV})$ and the $3d_{5/2}(M_V)$ transition range of CeO_2.

Slight sputtering of the AR CeO_2 caused its partial reduction into trivalent and metallic Ce states, as indicated by XPS and ELS. It is assumed that preferred sputtering of the oxygen ions causes this behavior, as reported for uranium oxide.[12] Therefore, sputtering of the CeO_2

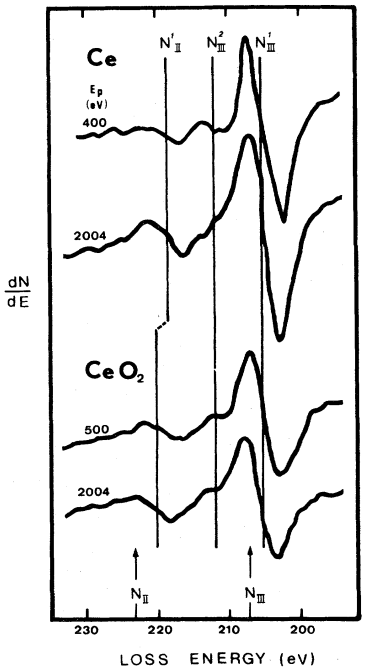

FIG. 9. Electron-energy-loss spectra near the $4p_{1/2}(N_{II})$ and the $4p_{3/2}(N_{III})$ transition range of SP Ce and CeO_2 for different incident electron energies.

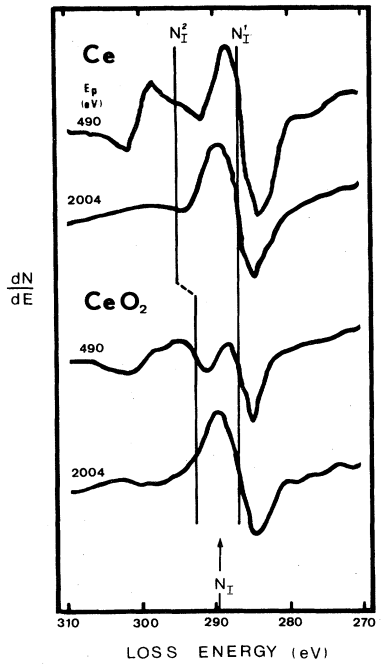

FIG. 10. Electron-energy-loss spectra near the $4s(N_I)$ transition range of SP Ce and CeO_2 for different incident-electron energies.

was avoided whenever possible and applied very carefully when it was absolutely necessary.

The position of a peak in the derivative spectra was taken as the midpoint between the local maximum and minimum. The peak positions given in the present work are the averages of measurements with different primary electron energies. The error ranges are standard deviations from the averages.

III. RESULTS AND DISCUSSION

The electronic scheme level of Ce metal[13] down to the -1185-eV, M_{III} level is illustrated on the right-hand side of Fig. 1. The levels are assigned by both electronic and spectroscopic notations. ELS of sputtered clean cerium metal and cerium dioxide were recorded at six different energy ranges according to this scheme, namely:

(1) The valence-band region, $\Delta E \leq 50$ eV.
(2) The $4d$ range, $90 \leq \Delta E \leq 150$ eV.
(3) The $4p$ range, $200 \leq \Delta E \leq 230$ eV.
(4) The $4s$ range, $280 \leq \Delta E \leq 300$ eV.
(5) The $3d$ range, $870 \leq \Delta E \leq 910$ eV.
(6) The $3p$ range, $\Delta E \simeq 1185$ eV.

In each range, different primary energies of the incident electrons (E_p) were applied, ranging from 3000 eV down to the threshold of the corresponding energy band. Some of the spectra are shown in Figs. 2—10. In some of these figures x-ray absorption spectra (cf. Figs. 4, 7, and 8) and XPS (cf. Fig. 7) are displayed for comparison with the present ELS results. The different line positions are summarized in Tables I—IV. Identified peaks, in most of the figures, are indicated by vertical lines. The transitions that are related to core-level excitations in cerium metal are illustrated on the left-hand side of Fig. 1 and are denoted by the spectroscopic notations of the origin core levels. The details of the final energy levels together with a calculated approximate shape of the conduction band of cerium metal[14] are plotted in Fig. 11. Within the valence-band region (Figs. 2 and 3) five peaks (P^1, P^2,S^1,S^2, and C) which are not related to core-level excitations were detected. These results will be discussed further and related to some other observations on rare-earth systems.[1,5,15]

TABLE I. Main energy losses in the near-elastic-scattering (valence-band) region of sputtered cerium metal and of cerium dioxide (in eV). CB and VB represent conduction band and valence band, respectively.

	Metal	Oxide	Assumed assignment
C	2.8±0.7		CB excitation
		4.8±0.4	VB → CB transition
S^1	7.9±0.4		surface plasmon
		8.4±0.4	
P^1	13.1±0.4	14.2±0.4	bulk plasmon
S^2	18.7±0.2		second surface plasmon
P^2	21.6±0.5	24.2±0.4	second bulk plasmon
O_{II}^1	28.0±0.4	30.6±0.4	$5p \rightarrow 4f$ transition
O_{II}^2	31.1±0.8		
O_I^1	36.9±0.4		$5s \rightarrow 4f$ transition
		46.0±1.0	

A. Excitations in metallic cerium

Lines P^1, P^2, S^1, and S^2 in Table I (Figs. 2 and 3) are related to different plasmon excitations. The plasmon excitations, which are collective excitations of the conduction electrons, are usually treated according to the free-electron model. The excitation energy of a bulk plasmon is given by this theory as[1,16]

$$\Delta Eb = \hbar(4\pi ne^2/m)^{1/2} , \quad (1)$$

where n is the electron density, and e and m are the charge and the mass of the free electron, respectively. Assuming three conduction electrons per Ce atom in the metal, Eq. (1) yields the value 11 eV, which is 2.1 eV below peak P^1. Similar shifts were obtained for other rare-earth elements.[1,3,5] In Sm the shift was only 0.8 eV.[6] A possible explanation to these shifts may be the contributions of the low-energy plasmons associated with divalent surface ions. The shifts may be attributed to the interband transitions with frequencies which are lower than the plasma frequency.[17]

The peak at 7.9 eV, S^1, is ascribed to the surface plasmon. The energy of a surface plasmon, ΔEs, is related to bulk plasmon by

$$\Delta Es = \Delta Eb/a \quad (2)$$

with $a = \sqrt{2}$ for smooth uniform surface and $a = \sqrt{3}$ for surface made of an agglomeration of small spheres.[18]

TABLE II. Peak energies (in eV) of the electron loss and x-ray absorption (Ref. 7) spectra near the threshold of the $4d$ excitation [at 110 eV (Ref. 13)] in sputtered cerium metal and cerium dioxide.

	Metal		Oxide	
	ELS	X-ray absorption	ELS	X-ray absorption
N_{IV}^{4}	127.7±0.9	124.3		
$N_{IV}^{4'}$			131.5±0.6	130.8
$N_{IV}^{4''}$			124.5±0.6	125.0
N_{IV}^{3}	121.4±0.3	121.5	121.2±0.5	
N_{IV}^{2}	110.2±0.3	111.5, 110.4[a]	110.2±0.8	
		105.8, 106.6		107.6, 108.2[a]
N_{IV}^{1}	104.0±0.3	103.5	104.5±0.8	103.4

[a]Only high-intensity absorption peaks are given for the near-threshold absorption spectrum.

Owing to the experimental conditions (sputtering) the latter is more likely to be the case in the present experiment, and using Eq. (2) one obtains the value $\Delta Es = 7.6$ eV, which is in good agreement with the 7.9 eV obtained. It is noteworthy that the intensity of this line is relatively high. The peaks at 18.7 eV, S^2, and 21.6 eV, P^2, are the second surface and bulk plasmons, respectively.

Peak C, at the low-energy side of the valence range (2.8 eV) is ascribed, by analogy to other rare-earth metals (Table V), to one-electron intraband excitation within the conduction band. The $4f$ excitation threshold of Ce lies 1.9 eV below the Fermi level.[19] Nevertheless, we exclude the identification of this line as a $4f$ excitation since in other rare-earth elements the $4f$ contributions to these transitions were found to be negligible. These transitions were not detected by transmission mode ELS, probably due to the lack of surface sensitivity of this technique.

All the other peaks displayed in the ELS are related to core-level excitations. For each excitation the transition can occur into three subgroups according to the location of the final energy states relative to the Fermi level; i.e., below, within, and above the Fermi level. The transitions related to the first subgroup display sharp narrow peaks, whereas transitions associated with the second subgroup, i.e., transitions to the vicinity of the Fermi level, show broadened and less intense peaks. The transitions of the third subgroup, with the final states which lie well above the Fermi level, display wide asymmetric line shapes.

The core-level excitations are interpreted as an electron transition from the relevant core level into the partially empty $4f$ level, or, in the case of the second subgroup, into the conduction band. The final electronic configurations for the different core-level excitations are given in the bottom of Fig. 11. For example, the excitations of the $4d$ core level, N_{IV}^{1}, N_{IV}^{2}, N_{IV}^{3}, and N_{IV}^{4}, are transitions from the ground state $3d^{10}4f(^2F_{5/2})$ into the excited configuration $3d^{9}4f^{2}$. Strong exchange interactions exist between the $4f$ electrons and the holes in the core level following the excitation processes. These interactions result in the splitting of the final configurations and the existence of several possible transitions below and above the Fermi level for each core-level excitation. Transitions into the levels which lie below E_F give rise to well-defined lines. The x-ray absorption spectra of the $4d$ excitations, for example, reveal many well-defined lines below the Fermi level[7] (cf. Fig. 4). The lower resolution of the ELS technique does not allow the separation of these peaks which were superimposed into one or two lines. The uppermost split terms are approaching the continuum, well above the Fermi level. The broadening and asymmetry of the lines associated with the transitions into these terms are explained by autoionization of the excited levels into

TABLE III. Peak energies (in eV) of the electron loss, x-ray photoelectron spectroscopy, and x-ray absorption spectra near the threshold of the $3d$ excitations in sputtered cerium metal and cerium dioxide.

	Ionization threshold[a]	Metal			Oxide		
		ELS	Absorption[b]	XPS	ELS	Absorption[c]	XPS[d]
						905.6	
M_{IV}^{1}		900.6±1.0	899.0	903.0	901.4±0.3	901.4	899.9
$3d_{3/2}$	901.3		898.0				
M_{IV}^{2}		897.9±1.0	896.4		898.0±0.1		
M_{V}^{1}		882.8±0.9	882.2	884.5	883.4±0.4	883.7	881.6
$3d_{5/2}$	883.3		881.5			881.8	
M_{V}^{2}		878.0±1.0	879.3		879.1		

[a]Reference 15.
[b]Reference 9.
[c]Reference 1.
[d]Reference 30.

TABLE IV. Loss energies of the main peaks and excitation thresholds (Ref. 13) of the $4p$, $4s$, and $3p_{3/2}$ levels in sputtered cerium metal and cerium dioxide.

Level	Ionization threshold	Line	Metal	Oxide
$4p_{3/2}$	207.2	N^1_{III}	205.0±1	205.7±0.6
		N^2_{III}	212.0±1	212.2±0.7
$4p_{1/2}$	223.3	N^1_{II}	218.5±1	219.8±0.8
$4s$	289.6	N^1_{I}	287.0±1	287.0±0.8
		N^2_{I}	296.0±1	292.6±1.0
$3p_{3/2}$	1185.4	M^1_{III}	1180.0±2	1181.7±1.1

TABLE V. Loss energies of one-electron excitations in the valence range for some rare-earth metals.

Element	Loss energy (eV)	Reference
$_{58}$Ce	2.8	This work
$_{62}$Sm	2.6	6
$_{68}$Er	3.5	3
	5	
$_{70}$Yb	4	5
$_{71}$Lu	2.6	15
	5.5	

the continuum.[20] The lines of the second subgroup are also broad but less intense due to the width of the final conduction band.

Similar x-ray absorption and ELS were obtained for other rare-earth elements.[2,21,22] Recently, measurements of Ce levels were performed by the synchrotron radiation technique,[23] yielding results which are similar to ours. A theoretical effort was made to quantitatively calculate the absorption spectrum of the $4d^{10}4f \rightarrow 4d^9 4f^2$ transition in Ce metal.[10] The calculated levels range from 103.5 to 123.3 eV (the absolute scale was adjusted). The exchange interactions between the $4d$ hole and the $4f$ electrons are expected to be stronger than the exchange interactions between the $4f$ electrons and other level holes in the Ce. This fact is demonstrated by the spread of the final levels in Fig. 11. It is 23 eV for the $4d$ excitations ($4d^9 4f^2$ configuration), 18 eV for the $3d$ excitations ($3d^9 4f^2$ configuration), 14 eV for the $4p$ excitations ($4p^5 4f^2$ configuration), and 12 eV for the $4s$ excitations ($4s\,4f^2$ configuration). It is also reflected by the intensities of the corresponding transitions. For weaker exchange interactions fewer terms are located above the Fermi level, giving rise to lower transitions intensities. Thus the $4d$ excitations of the third subgroup are characterized by intense peaks (N^3_{IV}, N^4_{IV}) (occasionally referred to as "giant resonances") whereas lower intensity peaks (M^3_V, M^3_{IV}) are found for the third subgroup transitions of the $3d$ excitations and even lower for the $4p$ and $4s$ excitations.

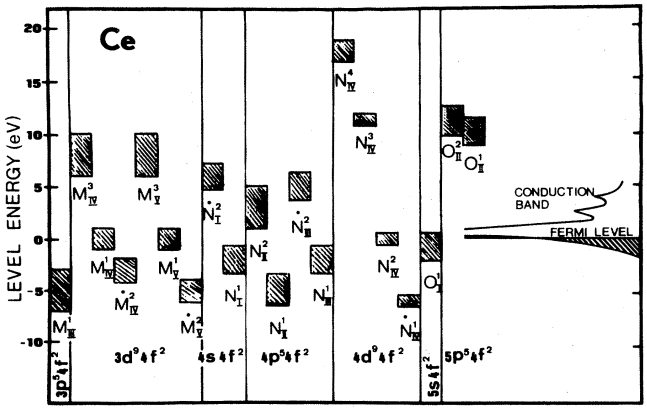

FIG. 11. Final energy levels related to the electron-energy-loss transitions together with a theoretical shape of the Ce conduction band (Ref. 8). A point above the peak notation indicates a dependence of the intensity of the transition on the energy of the incident electrons.

B. Transitions in CeO_2

Comparison between the ELS of metallic cerium and of cerium dioxide indicates that some of the peaks are sensitive to the chemical nature of the surface. The most significant difference is the disappearance of the surface plasmons S^1 and S^2. This is expected since there are no conduction electrons in the oxide. It makes the surface plasmon an excellent probe for the oxidation process of the metallic surface. On the other hand, "plasmonlike" peaks appear at somewhat higher energies, 14.2 and 24.2 eV. The appearance of plasmonlike peaks for the oxide is common to other rare earths and related systems. Their energies are 14 eV for the light rare earths La (Ref. 24) and Sm (Ref. 25) and lie between 15 and 16 eV for the heavier rare-earth oxides.[1,5] Occasionally Eq. (1) is applied to these line positions with the assumption of a "quasi-free"-electron model for the valence bands of the oxides. Such calculations yielded approximately 4 electrons per oxygen atom for the heavy rare-earth oxides and 5.3 electrons for EuO.[4] The same calculations yielded only 2.8 electrons per oxygen atom for CeO_2. This seems to violate the validity of the quasi-free-electron approximation in these cases. The assumption that these plasmonlike features are related to interband transitions from the O $2p$ level to an empty d-type band located above the metallic conduction band is more likely.

Another difference between the oxide and the metal is the shift towards higher energies which occurs for the other valence-band region transitions in the oxide. Thus for example, the $5p \rightarrow 4f$ transition (peak O^1_{II}) is shifted 2.6 eV, which is relatively a large shift as in comparison to other rare-earth systems [where the maximum reported shift is 1.3 eV, for Gd (Ref. 1)]. The transition which is correlated to peak O^1_I is shifted by an even higher energy value (9.1 eV). (It should be mentioned that this peak is the only one that has a different shape and intensity ratio for the AR Ce and the AR CeO_2.) We ascribe it to the $5s \rightarrow 4f$ transition as in the metal. Although its final energy lies well above the Fermi level, the very big chemical shift is quite surprising.

At the low-energy range we find for the oxide a transition at 4.8 eV. This line can be attributed to a valence-to-conduction band transition of an electron that belongs to the oxygen atom. The O $2p$ valence level in CeO_2 is found 5 eV (Ref. 26) or 6 eV (Ref. 27) below the Fermi level, in agreement with this assumption. Also at low primary electron energies, when the spectra is mainly due to the surface contamination overlayer, the peak at 4.8 eV dominates the spectrum, which confirms the assignment of this peak to the O $2p$ transition.

In addition to the valence-band region, two peaks of the core-level excitations exhibit a pronounced chemical dependence. Peak N_{IV}^4 of the $4d$ excitations in the metal is replaced by two other peaks, $N_{IV}^{4'}$ and $N_{IV}^{4''}$ (Figs. 5 and 6 and Table II). Peak N_I^2 of the $4s$ excitations is shifted towards higher energies (Table IV). It is possible that the sensitivity of these transitions to the chemical environment is due to the location of the corresponding final states which lie well above the Fermi level. By analogy to these results, one would expect to detect chemical shifts also for the other core-level transitions into the final states which lie above the Fermi level (i.e., the third subgroup transitions). However, the intensities of these peaks are very small and chemical shifts could not be detected. It is noteworthy that the chemical sensitivity of the $4d$ transitions of the third subgroup (i.e., into final state above the Fermi level) has been found only for the light rare earths,[7,8,28] not for the heavy ones.

C. Energy dependence of the transitions intensities

For metallic cerium the relative intensities of the peaks in the valence-band region which were not related to core-level excitations depend on the energy of the primary electron beam. In order to illustrate this dependence, the intensity ratios of the peaks P^1, S^1, and C to that of peak O_{II}^1 are plotted in Fig. 12 as a function of the primary energy of the incident electrons. Peak O_{II}^1 has been chosen as the reference because its intensity (normalized to the intensity of the elastic peak) was almost unchanged through all the primary energy range. The energy dependence of the ratio between the intensity of the surface plasmon to that of the bulk plasmon, S^1/P^1, is also plotted in Fig. 12. As indicated by this figure, the energy dependence is very pronounced below about 500 eV. In this range the intensity of the bulk plasmon has a minimum around 270 eV, whereas that of the surface plasmon exhibits two maxima. The intensity ratio of the surface to bulk plasmon exhibits a sharp maximum at 270 eV. Above about 1000 eV the peak intensities become almost independent from the primary energy of the incident electrons. The resemblance between the curves S^1/O_{II}^1 and C/O_{II}^1 may indicate that the interband excitations (C transitions) are into surface states.

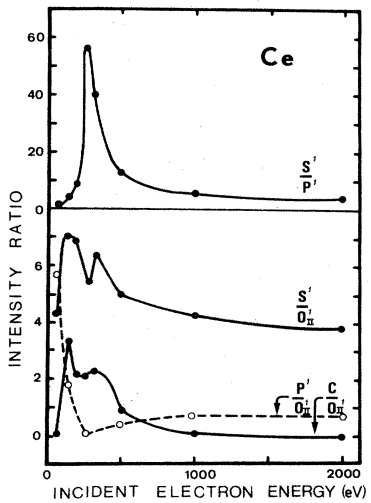

FIG. 12. Dependence of the intensity ratios of several peaks in the valence-band region on the incident-electron energy.

Five of the transitions that are related to core-level excitations exhibit primary energy dependence both in cerium metal and in cerium dioxide. These lines are denoted in Fig. 11 by points which appear above the corresponding line notations. Three of these lines, N_{IV}^1, M_V^2, and M_{IV}^2 (Figs. 4, 5, 7, and 8) belong to the first subgroup, i.e., their final state lies below the Fermi level and the other two, N_{III}^2 (Fig. 9) and N_I^2 (Fig. 10), belong to the third subgroup. The transition N_{IV}^3 (Fig. 5) exhibits energy dependence only in the oxide. The general trend in these peaks is a strong enhancement of the intensities with decreasing primary energy. A possible explanation of this trend is that the lines N_{III}^2 and N_I^2, which were related to $p \rightarrow f(\Delta l = 2)$ and $s \rightarrow f(\Delta l = 3)$ electron transitions, are optically forbidden. For incident electrons with energies well above the excitation threshold, the electron-energy-loss process (as well as x-ray absorption effects) can be accounted for in terms of dipole (optical) transitions. For low primary energies, however, multipole transitions of higher order take place.[29] This increases the probability of the optically forbidden transitions. For the N_V^1, M_V^2, and M_{IV}^2 lines which are related to $d \rightarrow f$ ($\Delta l = 1$) transitions (though optically allowed), the addition of higher multipole terms at low primary energies increases the transition probabilities. Such behavior was also observed in ELS of the $3d$ transitions in GaAs and in Ge for primary energies below 100 eV.[29] However, it seems that for cerium the higher multipole transitions contribute at higher primary energies. It is noteworthy that while the $\Delta l = 1$ transitions which are affected by the primary energy variation are associated with final states below the Fermi level (i.e., the first subgroup), the corresponding $\Delta l = 2,3$ transitions are associated with final states above the Fermi level.

IV. CONCLUSIONS

Using the ELS technique we measured various excitations for metallic sputtered cerium and as-received cerium dioxide. Within the valence-band region we found collective transitions, i.e., plasmons, typical of the metallic state. For the oxide the surface plasmons disappeared and the bulk plasmons shift to higher energies, displaying plasmonlike peaks. These plasmonlike peaks were attributed to interband transitions from the O $2p$ level into an empty d-type band.

Core-level excitations for metallic cerium are summa-

rized in Fig. 1. The details of the final states are summarized in Fig. 11. Owing to exchange interactions, the terms of the final states are widely spread around the Fermi level. Therefore the core-level excitations were divided into three subgroups according to the position of the final states as follows:

(a) Levels below the Fermi level. These are almost localized levels and give rise to narrow peak shapes.

(b) Levels in the vicinity of the Fermi level. The $4f$ terms in this region overlap the conduction band. The line shapes of these transitions may, therefore, be broadened and less intense.

(c) Levels above the Fermi level. The transitions into these levels produce wide and asymmetric line shapes due to autoionization processes.

The transitions associated with the third subgroup are the most sensitive towards chemical changes (i.e., they display the largest chemical shifts in the oxide) due to the unscreened nature of the corresponding final states. Some of the ELS peak intensities (e.g., the plasmons and some of the core-level excitations) depend on the primary energy of the incident electrons. However, for primary energies above about 1000 eV this dependence becomes weak and the intensities are almost unaffected by the primary energy variations.

[1]C. Colliex, M. Gasgnier, and P. Trebbia, J. Phys. (Paris) **37**, 397 (1976).

[2]P. Trebbia and C. Colliex, Phys. Status Solidi B **58**, 523 (1973).

[3]E. Bertel, F. P. Netzer, and J. A. D. Matthew, Surf. Sci. **103**, 1 (1981).

[4]A. Nigavekar and J. A. D. Matthew, Surf. Sci. **95**, 207 (1980).

[5]E. Bertel, G. Strasser, E. P. Netzer, and J. A. D. Matthew, Surf. Sci. **118**, 387 (1982).

[6]E. Bertel, G. Strasser, E. P. Netzer, and J. A. D. Matthew, Phys. Rev. B **25**, 3374 (1982).

[7]R. Hansel, P. Rabe, and B. Sonntag, Solid State Commun. **8**, 1845 (1970).

[8]S. Suzuki, T. Ishii, and T. Sogawa, J. Phys. Soc. Jpn. **38**, 156 (1975).

[9]C. Bonnele, R. C. Karnatak, and J. Sugar, Phys. Rev. A **9**, 1920 (1974).

[10]J. L. Dehmer, A. F. Starace, U. Fano, J. Sugar, and J. W. Casper, Phys. Rev. Lett. **26**, 1521 (1971); A. F. Starace, Phys. Rev. B **5**, 1773 (1972); J. Sugar, *ibid.* **5**, 1785 (1972); J. L. Dehmer and A. F. Starace, *ibid.* **5**, 1792 (1972).

[11]T. L. Barr, in *Quantitative Surface Analysis of Materials,* edited by N. S. McIntyre (American Society for Testing Metals, Philadelphia, 1978), Spec. Tech. Publ. No. 643, p. 83.

[12]B. W. Veal and D. J. Lam, Phys. Lett. **49A**, 466 (1974).

[13]J. A. Bearden and A. F. Burr, Rev. Mod. Phys. **39**, 125 (1967).

[14]E. A. Kmetko, in *Electronic Density of States,* Natl. Bur. Stand. (U.S.) Spec. Publ. No. 323, edited by L. H. Bennet (NBS, Washington, D.C., 1971), p. 67.

[15]J. Onsgaard, S. Tougaard, P. Morgen, and F. Ryborg, in *Proceedings of the Fourth International Conference on Solid Surfaces, and the Third European Conference on Surface Science, Cannes, France, 1980,* edited by D. A. Degras and M. Costa (Societe Francaise du Vide, Paris, 1980), Vol. II, p. 1361; B. Brousseau-Lahaye, C. Colliex, J. Frandon, M. Gasgnier, and P. Trebbia, Phys. Status Solidi B **69**, 257 (1975).

[16]D. Bohm and D. Pines, Phys. Rev. **92**, 609 (1953); D. Pines, *ibid.* **92**, 626 (1953).

[17]H. Raether, *Excitation of Plasmons and Interband Transitions by Electrons,* Vol. 88 of *Springer Tracts in Modern Physics* (Springer, Berlin, 1980), Chap. 2.

[18]R. H. Ritchie, Phys. Rev. **106**, 874 (1957).

[19]A. Platau, A. Callenas, and S. E. Karlsson, Solid State Commun. **37**, 829 (1981).

[20]C. Kunz, in *Optical Properties of Solids—New Developments,* edited by B. O. Seraphin (North-Holland, Amsterdam, 1979), Chap. 10.

[21]T. M. Zimkina, V. A. Fomichev, S. A. Griborski, and I. I. Zhukova, Fiz. Tverd. Tela (Leningrad) **9**, 1447 (1967) [Sov. Phys.—Solid State **9**, 1128 (1967).]

[22]V. A. Fomichev, T. M. Zimkina, S. A. Gribovski, and I. I. Zhukova, Fiz. Tverd. Tela (Leningrad) **9**, 1490 (1967) [Sov. Phys.—Solid State **9**, 1163 (1967).]

[23]L. I. Johansson, J. W. Allen, T. Gustafsson, I. Lindau, and S. B. M. Hagström, Solid State Commun. **28**, 53 (1978).

[24]Unpublished data taken in our laboratory.

[25]G. Dufor, R. C. Karantak, J. M. Mariot, and C. Bonelle, Chem. Phys. Lett. **42**, 433 (1976).

[26]C. R. Helms and W. E. Spicer, Appl. Phys. Lett. **21**, 237 (1972).

[27]A. Piatau and S. E. Karlsson, Phys. Rev. B **18**, 3820 (1978).

[28]H. W. Wolff, R. Bruhn, K. Badler, and B. Sonntag, Phys. Lett. **59A**, 67 (1976).

[29]R. Ludeki and A. Koma, Phys. Rev. Lett. **34**, 817 (1975).

[30]*Handbook of X-Ray Photoelectron Spectroscopy,* edited by C. D. Wagner, W. M. Riggs, L. E. Davis, J. F. Maulder, and G. E. Muilenberg (Perkin-Elmer Co., Eden Prary, 1979), p. 134.